Original Research

Exploration of the active components and pharmacological mechanism of Compound Longmaining for the treatment of myocardial infarction

Jia Li[1,†], Xiao Wang[1,†], Diaodiao Bu[1,†], Junbo Zou[1], Shining Xun[2], Yao Wang[1], Yanzuo Jia[1], Shangshang Yu[1], Wenfei Wang[1], Jiahui Zheng[1], Jiejun Hou[2], Xiaofei Zhang[1,*], Changli Wang[1,*]

[1]*Department of Pharmaceutics, College of Pharmacy, Shaanxi University of Chinese Medicine, 712000 Xianyang, Shaanxi, China,* [2]*Affiliated Hospital of Shaanxi University of Chinese Medicine, 712000 Xianyang, Shaanxi, China*

TABLE OF CONTENTS

Submitted: 22 April 2021 Revised: 10 August 2021 Accepted: 20 August 2021 Published: 30 October 2021

1. Abstract

Background: Myocardial Infarction (MI) is a cardiovascular disease with a high morbidity and mortality rate. While MI is currently treated with pharmaceuticals, there is a need for new treatment options: compound Chinese medicines may have unique advantages for the treatment of MI. **Methods**: A combination of network pharmacology and experimental verification is used to identify the ingredients and mechanism of Compound Longmaining (CLMN) for treating MI. Network pharmacology combined with the gene expression omnibus (GEO) chip method is used to analyze the primary pathway of CLMN for treating MI, and then molecular docking is used to verify the affinity of key target proteins in the primary pathway that bind to active molecules. The major active compounds of CLMN are screened using the docking score results. The CIBERSORT algorithm is used to evaluate immune cell infiltration in MI, and high performance liquid chromatography (HPLC) is used to control the quality of the components. Finally, a mouse model is established to verify the molecular mechanism of CLMN for treating MI using hematoxlyn eosin (HE) staining and immunohistochemistry. **Results**: By utilizing network pharmacology combined with molecular docking, the mechanism of action of CLMN for the treatment of MI was found to possibly be related to the ingredients of puerarin, daidzein, ferulic acid, chrysin, and galangin. These molecules regulate the NF-Kappa B signaling pathway and the expression of *RELA*, *IKBKB*, *NKBIA*, and other targets. The CIBERSORT algorithm and ggplot2 package analysis were used to distinguish the immune cells, such as neutrophils, macrophages, and T cells, that play a key role in the development of MI. HPLC controlled the quality of the screened medicinal ingredients. An immunohistochemical analysis showed that the *TNF-*α and *TRAF-2* expression levels in MI of the CLMN-treated mice were decreased, while *IkB*α was increased. HE staining showed CLMN reduced inflammation in mouse cardiomyocytes and decreased fibrosis. **Conclusions**: This study showed that CLMN treatment of MI is a process that involves multi-components, multi-targets and multi-pathways, and the established multi-index component content measurement of the CLMN decoction can be used for quality control of CLMN.

2. Introduction

Cardiovascular disease is the leading cause of death among urban and rural residents in China, a trend that has increased recently [1]. In 2014, there were approximately 290 million patients with cardiovascular disease, which included 2.5 million myocardial infarction cases. In the United States, there are approximately 1.5 million cases of MI annually with a yearly incidence rate of approximately 600 cases per 100,000 people [2]. Although the prognosis of MI has been greatly improved, it is still the primary cause of morbidity and mortality in the world [3]. Therefore, it is important to continue to develop new therapeutics based upon the use of novel strategies to understand the mechanisms involved in MI. Following MI, there is cardiomyocyte necrosis, the result of ischemia that causes an inflammatory response. Oxidative stress mediated by inflammatory factors damages vascular endothelial cells, and leads to plaque rupture and hemorrhage [4]. These triggering events cause serious clinical manifestations.

Traditional Chinese Medicines (TCMs) have the potential advantage of low toxicity and broad spectrum activity to prevent and treat a wide variety of diseases including MI. CLMN is composed of the following natural ingredients: *Pueraria lobata*, *Dioscoreae nipponica Makino*, *Ligusticum wallichii*, and propolis. The active molecules identified in CLMN are flavonoids, puerarin, alkaloids, lactones, phenols, organic acids, steroidal saponins, flavonoids and terpenes [5]. The CLMN is an in-hospital preparation developed by Professor Tao Genyu of the affiliated Hospital of the Shaanxi University of Chinese Medicine. Since previous studies have confirmed that the CLMN decoction has a significant therapeutic effect on MI [6], we used network pharmacology combined with a gene expression omnibus (GEO) chip analysis and molecular docking to explore which components, targets, and pathways that are regulated by CLMN.

Network pharmacology can provide insight into "component-target-pathways" of drugs and help predict the correlation between drugs and diseases [7]. The microarray analysis has been widely used to identify differentially expressed genes (DEGs) and functional pathways involved in disease progression. Finally, molecular docking is a technique used to visualize drug interactions with target proteins [8]. This study explores the possible mechanism of CLMN for the treatment of myocardial infarction and uses the CIBERSORT algorithm to evaluate the immune cell infiltration in MI from the GEO database. This study also uses the high performance liquid chromatography (HPLC) method to establish the quality control of CLMN and conduct an animal experiment verification to provide a more reliable basis for clinical application. The flow chart of the study is shown in Fig. 1.

3. Materials and methods

3.1 Screening of chemical constituents and acquisition of targets of CLMN

The Traditional Chinese Medicine Systems Pharmacology (TCMSP, http://lsp.nwu.edu.cn/tcmsp.php) database [9] and scientific literature allowed us to identify the chemical constituents of CLMN and the targets of four TCMs: *p. lobata*, *D. nipponica Makino*, *L. wallichii*, and propolis. The oral Bioavailability ((OB) $\geq$30%) and

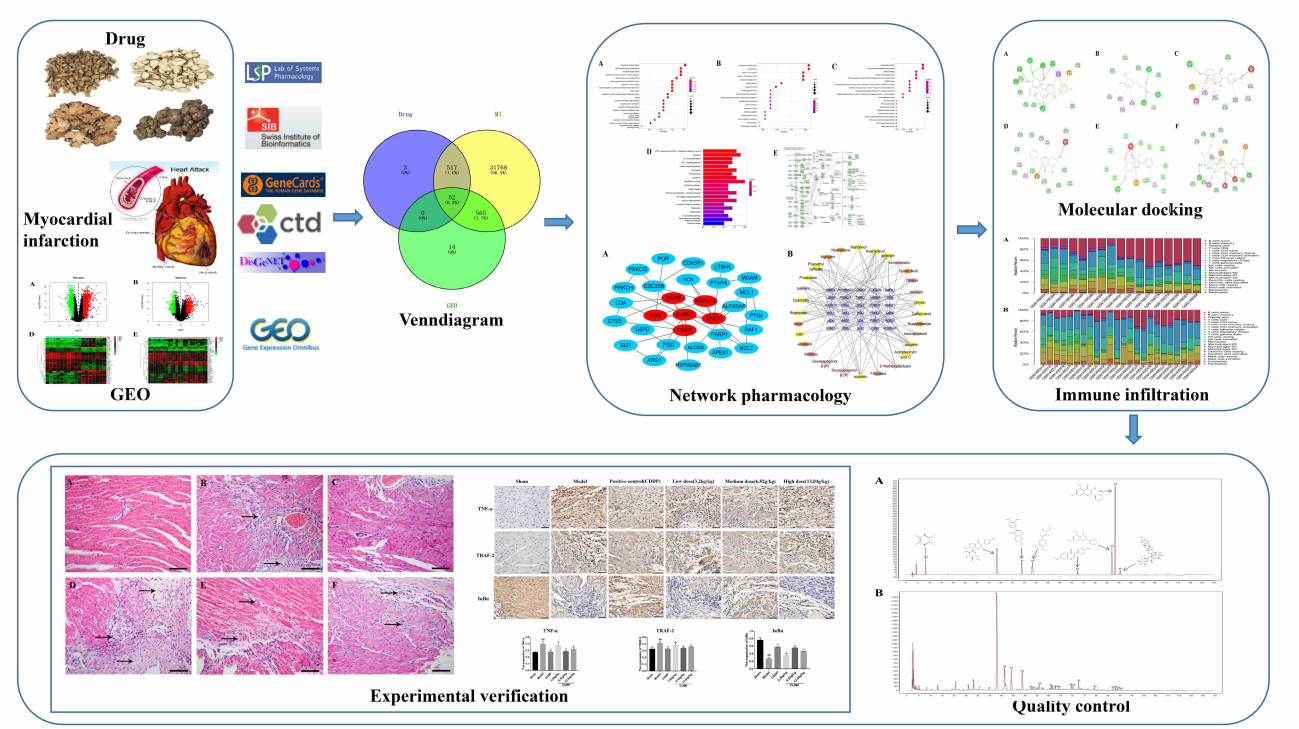

Fig. 1. A detailed flow chart of the study.

drug-likeness ((DL) ≥0.18) [10] parameters were used for screening. The target obtained from the TCMSP database was imported into the Uniprot (https://www.uniprot.org/) database [11] and standardized using its official name. The 2D structure of the active components were downloaded from the PubChem (https://pubchem.ncbi.nlm.nih.gov/) database [12] and the targets were predicted using the Swiss Target Prediction (https://www.swisstargetprediction.ch/) database [13]. The targets obtained from the TCMSP database and the Swiss Target Prediction database were merged, and the duplicates were removed, and this resulted in the chemical component target of CLMN.

3.2 Acquisition of disease targets

In order to obtain gene data related to MI, we searched GeneCards (https://www.genecards.org/) [14], Comparative Toxicogenomics Database (http://ctdbase.org/http://ctdbase.org/), and the DisGeNET (https://www.disgenet.org/) public database using the keyword "Myocardial Infarction". The GSE61145 (GPL6106) and GSE60993 (GPL6884) gene expression datasets were downloaded from the GEO (https://www.ncbi.nlm.nlh.gov/geo/) database [15], and 10 normal samples and seven preoperative MI samples in GSE61145 were chosen. In addition, seven normal samples and 17 MI samples in GSE60993 were collected from the peripheral blood of the subjects. Using the R language "limma" package [16] on the analyses and the expression of genes after normalization, screening disease DEGs, and map volcano, the screening conditions were determined to be a p-value ≤ 0.05 and a $|\log FC| \geq 0.5$ to screen out the DEGs of diseases. Using the "pheatmap" package [17], the first 20 genes identified by the most significant up-regulation or down-regulation were obtained, and the heat maps were drawn.

3.3 Gene mapping

The overlapped genes were deleted from the disease genes and component target genes obtained from the multiple databases. The genes that overlapped between the datasets were obtained using an online Venn analysis tool (https://bioinfogp.cnb.csic.es/tools/venny), and the common genes were screened by mapping.

3.4 Construction and analysis of the protein-protein interaction (PPI) network

The target genes of the CLMN components were introduced into the STRING (https://string-db.org/) database [18], and the research species was set to "Homo sapiens". In the setting, the highest confidence level was set to 0.9, the free target genes were hidden, and the TSV format file of the relationship diagram was derived after obtaining the target-protein interaction relationship. We imported the Tab Separated Values file into Cytoscape3.7.2 (Donnelly Centre for Cellular and Biomolecular Research, Toronto, North America, Canada) [19] and adjusted the color of the nodes according to the degree value, in order to more intuitively show the important CLMN targets.

3.5 Construction of the drug active ingredient-core target network

The target genes of the active components of CLMN were imported into Cytoscape 3.7.2. The node representing the drug active component was set to "source node", the node representing the disease target gene was set to "target node", and the network attribute was set to "interaction type" to draw the "drug active ingredient-core target" network.

3.6 Gene ontology (GO) and Kyoto encylopedia of genes and genomes (KEGG) enrichment analysis

The core target genes of drug-disease were transformed from Gene Symbol to entrezID, using R language, and the data was processed using "BiocManager". We used the R package clusterProfiler package [20] to perform the GO and KEGG enrichment analysis on the shared targets, The GO and KEGG enrichment analysis were obtained under the condition of $p < 0.05$.

3.7 Molecular docking

The protein structure of the key target was downloaded from the Protein Data Bank (PDB, https://www.rcsb.org/) database [21], and we download the sdf file for the ligand (active component and positive drug corresponding to the target) from the Pubchem database. The LibDock tool of Discovery Studio 4.0 software (Neo Trident Technology LTD, Beijing, China) was used to dock the key target protein with its corresponding active component and positive drug, and the score was analyzed.

3.8 CIBERSORT

Two microarray data sets, GSE61145 and GSE60993, were downloaded from the GEO database to screen different infiltrated immune cells, and the CIBERSORT algorithm [22] was used to evaluate the immune cell infiltration in MI. CIBERSORT is an analytical tool that represents the cellular composition of complex tissues based on pretreated gene expression profiles. This default signature matrix of 100 permutations was used in this algorithm, only data with p values < 0.05 were filtered and retained for the following analysis. From the CIBERSORT website (http://CIBERSORT.stanford.edu/) download of the LM22 gene file, 22 immune cell subgroups were used to define and analyze the MI peripheral blood expression data, and CIBERSORT was utilized to express the file p values and root mean square error count and immune cell data obtained. The R language ggplot2 package [23] was used to visualize the results.

3.9 Preparation of the CLMN decoction

The CLMN included four types of medicinal materials, namely *P. lobata*, *D. nipponica Makino*, *L. wallichii*, propolis. The *P. lobata*, *D. nipponica Makino*, *L. wallichii* decoction pieces were purchased from the Baoji Xiangyuan Traditional Chinese Medicine Decoction Pieces Co., LTD., and the propolis was purchased from the Natural Son Peak Products Co., LTD., Xianyang, Shaanxi Province. The CLMN decoction was prepared as described previously. A total of 18 g of *P. lobata*, 12 g of *D. nipponica Makino*, 12 g of *L. wallichii*, and 6 g of propolis was added to14 volumes of water, heated and then boiled twice. The filtrate was consisted of concentrates of 0.32 g the crude drug/mL [24].

3.10 Quality control of CLMN

By utilizing the network pharmacology, molecular docking technology and a literature review, the effective and high content of the pharmacodynamic components in the CLMN were determined, and HPLC was used to control the quality of the effective components.

3.11 Experimental methods

3.11.1 Experimental animals

Male Balbc mice weighing 22–28 g and 10–14 weeks old were purchased fromthe Chengdu Dashuo Experimental Animal Co., Ltd., Chengdu, China. The experimental animal license number was SYXK (chuan) 2020-030. The animals were maintained under the standard laboratory temperature and humidity conditions and had free access to food and water throughout the study. This experiment was approved by the Animal Ethics Committee of the Shaanxi University of Chinese Medicine.

Sixty mice were randomly divided into six groups: a sham operation group, a positive control: a Compound Danshen Dropping Pills (CDDP) group, an MI model group, and low-dose, medium-dose and high-dose CLMN groups. The mice in the sham operation group and the MI model group were given normal saline. The mice in the CDDP group were given 9.78 g/kg/d, and the mice in the CLMN groups were given the CLMN decoction at 3.26 g/kg/d (low dose), 6.52 g/kg/d (medium dose) and 13.04 g/kg/d (high dose) for seven days.

3.11.2 The MI mouse model

The MI model was established as described previously. Briefly, we opened the pericardium and located the left anterior descending coronary artery and inserted a needle. Then the coronary artery of the left anterior descending branch of the left atrium was ligated using a 8/0 monofilament polypropylene suture. This resulted in permanent ischemia of the artery below the ligation line. For the sham group, the needle was inserted into the left anterior descending branch of the coronary artery without ligation after thoracotomy [25, 26].

3.11.3 Tissue collection & HE staining

Following MI, the mice were anesthetized and the fresh heart tissue was quickly removed and frozen in liquid nitrogen for the pathological examination. The myocardial tissue was then fixed in 4% paraformaldehyde and embedded in paraffin. Thereafter, the tissue was cut into 5 um

thick sections and stained using hematoxylin-eosin (HE), and the histopathological examination was performed under a light microscope (OLUMPUS Japan) at 200 magnification.

3.11.4 Immunohistochemical analysis

The myocardial tissue was cut into 5 um slices, placed in xylene, and hydrated with an ethanol gradient (100%, 95%, 80%, 70%, and pure water). After antigen repair, the slices were incubated in H_2O_2 for 15 m in the dark, and the primary antibody was diluted using 5% bovine serum albumin (dissolved in phosphate buffering solution). The slices were incubated at 4 °C overnight. The following day, the second antibody was added and incubated at room temperature for 30 min, and then washed with PBS for three times (5 m each). DAB-H_2O_2 was then used until the color developed. The slices were then incubated in hematoxylin for 2 m, washed with water, differentiated with hydrochloric acid and ethanol for 3 s, washed with running water for 15 m, and dehydrated. The expressions of *TNF-*α, *TRAF2* and IkBα were evaluated using quantitative grayscale scanning with a medical image analysis system after taking pictures under a high magnification visual field (400×).

3.11.5 Statistical analysis

Data was analyzed using SPSS Statistics 26 software (IBM Corp., Chicago, IL, USA), and the results are expressed as means ± SDs. When the variance was homogeneous, a one-way analysis of variance was used to analyze the mean between the groups, and a $p < 0.05$ was statistically significant.

4. Results

4.1 Collection of the CLMN active ingredients and targets

In this study, 37 active compounds were collected from the TCMSP and PubChem databases, including nine active compounds in *P. lobata* targeting 506 proteins, four active compounds in *D. nipponica Makino* targeting 109 proteins, 12 active compounds in *L. wallichii* targeted 443 proteins, and 12 active compounds in propolis targeting 1219 proteins. After removing the same target of four herbs, a total of 572 target proteins of CLMN were obtained.

4.2 Collection of disease targets

Using the Gene Cards, CTD, and DisGeNET databases in combination, a total of 32,902 MI-related targets were obtained after the deletion of duplicate and invalid targets. A total of 1764 and 1079 significant difference genes were obtained by analyzing the GSE61145 and GSE60993 chips, respectively, and the DEGs volcanic map was drawn. As shown in Fig. 2. We examined the expression of DEGs from both datasets. Genes that were highly or lowly expressed in both datasets were retained as DEGs, resulting in 631 DEGs.

4.3 Screening core targets

There were 572 compositional targets from the TCMSP and Swiss Target Prediction databases, 32,902 disease targets from the GeneCards, CTD and DisGeNET databases, and 631 DEGs from the GEO database that were imported into an online Venn analysis tool. A total of 52 drug-disease interaction targets were obtained. The results are shown in Fig. 2C.

4.4 Protein interaction network (PPI) analysis

The 52 targets described above were imported into the STRING database and were viewed in the network diagram "Analysis" of the database. The PPI network consisted of 52 nodes and 37 edges. The average node degree was 1.42, and the average clustering coefficient was a *p*-value $< 8.04 \times 10^{-9}$, that indicated that the target genes had potential interactions. The TSV file data of protein interactions were obtained, and then the data was imported into the Cytoscape software to construct the protein interaction network diagram, as shown in Fig. 3A. The "Network Analyzer" tool was used to score the proteins. In the Figure, the top 6 proteins are represented by a red oval, and the rest are represented by a blue oval. *MAPK1*, *STAT3*, *TIMP2*, *MMP9*, and other proteins with high scores play an important role in the regulation of the network and are the key targets of CLMN for the treatment of MI.

4.5 Construction of the "active ingredient-core target" network

Using the "merge" tool within the Cytoscape3.7.2 software (Donnelly Centre for Cellular and Biomolecular Research, Toronto, North America, Canada), a network diagram for the 37 drug active components and 52 MI targets was constructed (Fig. 3B). Among them, the ovals of the different colors were used to represent each active ingredient from different TCMs, and the triangle represents the disease targets. The network consists of 159 nodes and 125 edges. From the graph, it is apparent that a single active component corresponds to multiple targets, and one target can also correspond to multiple active components. Taken together, CLMN therapy for MI has the characteristics of possessing multi-components and multi-targets. Using the Network Analyzer analysis tool, the top components were galangin, apigenin, phenethyl caffeate, and acacetin, and the top targets were *ALOX5*, *MMP9*, *CDK5R1*, *ARG1* and *BCL2*. This result suggested that all may play an important role in the mechanism of CLMN for the treatment of MI.

4.6 GO and the KEGG enrichment analysis

According to a $p < 0.05$, the GO and KEGG enrichment analysis were performed on 52 selected common targets using R language. It was found that CLMN primarily treated MI through a cellular response to chemical stress, a response to oxidative stress, regulation of reactive oxygen species metabolic processes, and other aspects in the

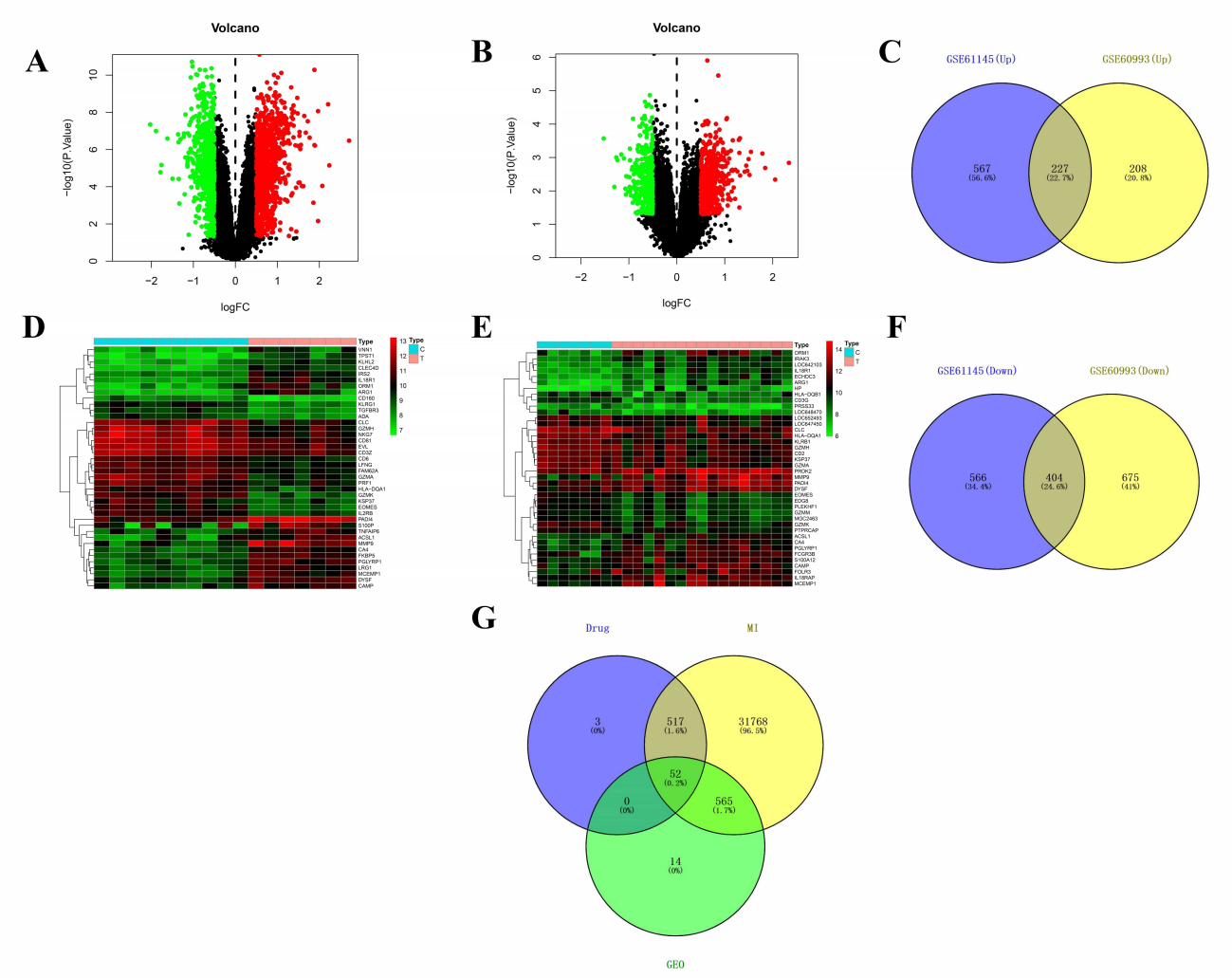

Fig. 2. Screening of core targets. (A) DEGs volcanic map of the GSE61145 chip. (B) DEGs volcanic map of the GSE60993 chip. (C) GSE61145 chip and GSE60993 chip up-regulate intersection genes. (D) DEGs heat map of GSE61145 chip. (E) DEGs heat map of GSE60993 chip. (F) GSE61145 chip and GSE60993 chip down-regulate intersection genes. (G) CLMN active ingredient target and disease target Venn diagram. In the volcano map, the down-regulated genes in the normal group are represented by green dots, while those up-regulated in the experimental group are represented by red dots.

biological process of CLMN. When $p < 0.05$, a total of 85 KEGG pathways were enriched. After removing the pathways not associated with the disease, 16 enrichment pathways that may be closely related to CLMN in treating MI were obtained from the top 50 pathways: the Apoptosis, Th17 cell differentiation, HIF-1, Necroptosis, NF-Kappa B, Lipid and atherosclerosis, Fc Epsilon RI, FoxO Signaling pathway, Th1 and Th2 cell differentiation, IL-17, JAK-STAT, TNF, PI3K-Akt signaling pathway, Fluid shear stress and atherosclerosis, Toll-like and Nod-like receptor signaling pathway. Among them, Th17 cell differentiation, NF-Kappa B, Fc Epsilon RI, FoxO, IL-17, JAK-STAT, TNF, PI3K-Akt, Toll-Like signaling pathway, and Nod-like receptor signaling pathway are signaling pathways that are related to the inflammatory response and have been widely reported in the literature. It is not difficult to find that CLMN may act on the inflammatory pathway to treat MI through this analysis. Fig. 4 represents a drawing of the GO analysis bubble chart of CLMN (Fig. 4A–C), the KEGG pathway analysis bar chart of CLMN (Fig. 4D) and the NF-Kappa B signal pathway map enriched in the first place (Fig. 4E).

4.7 Molecular docking analysis

The docking results are shown in Table 1, and the interactions between them are shown in Fig. 5. In order to further illustrate the binding activity between the target protein and its corresponding compound, in this study, the key targets *RELA*, *IKBKB*, *NFKBIA*, and their corresponding compounds in the NF-Kappa B pathway were selected. Discovery Studio 4.0 software (Neo Trident Technology LTD, Beijing, China) was used for positive drug verification experiments and molecular docking. The higher the binding activity, the higher the score. The docking scores of the target protein and its corresponding small molecule com-

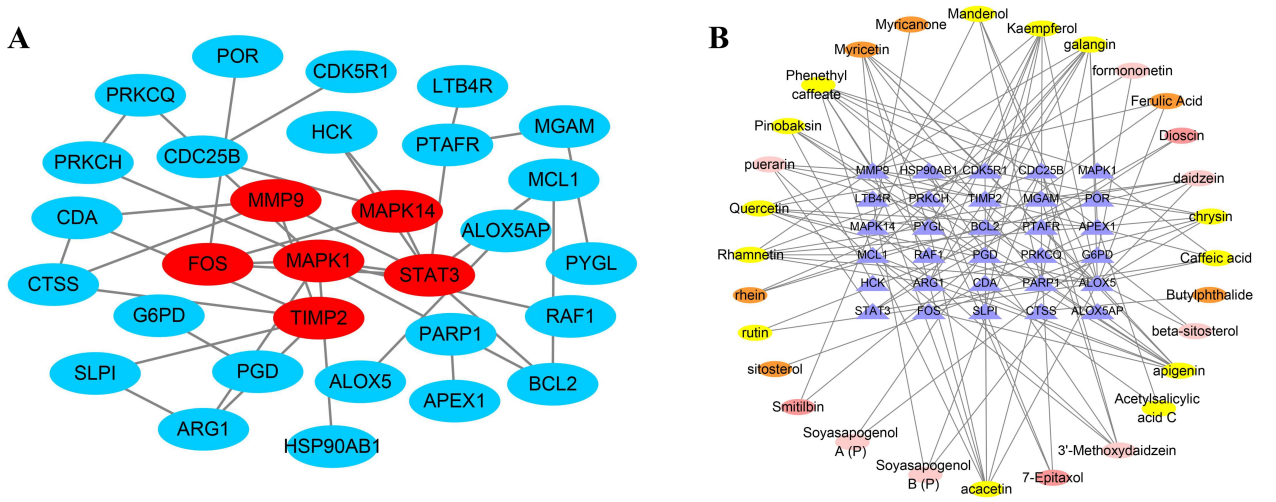

Fig. 3. CLMN-MI core target network diagram. (A) CLMN-MI core target PPI network diagram. (B) CLMN active component-core target interaction network diagram.

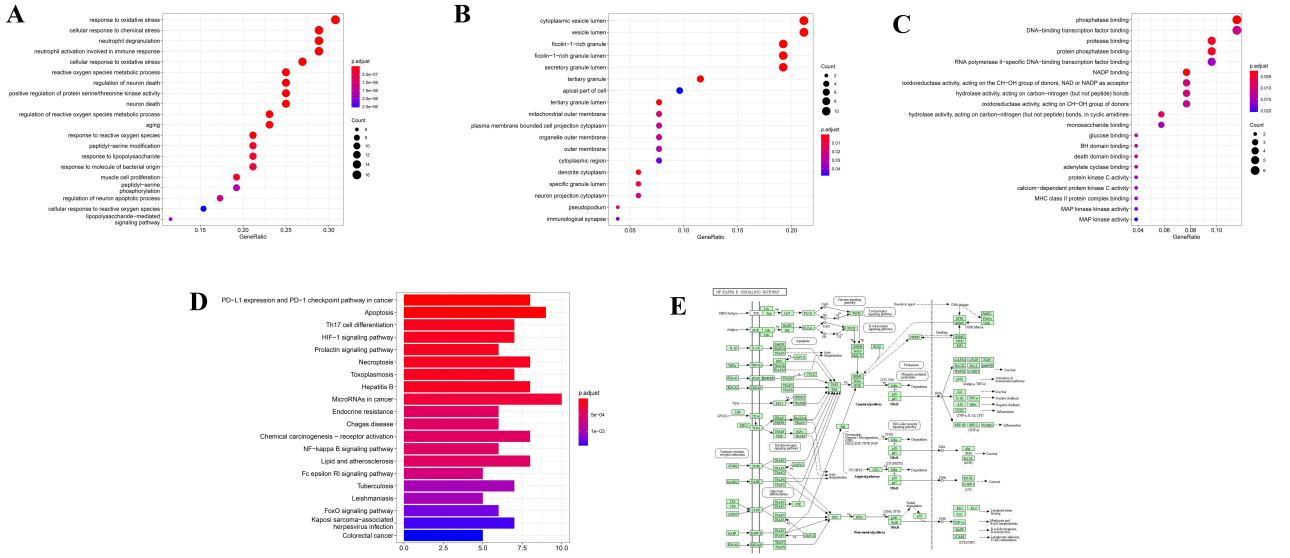

Fig. 4. GO analysis and KEGG pathway diagram of CLMN in the treatment of MI. (A–C) GO analysis bubble chart of CLMN treatment of MI. (D) KEGG pathway analysis histogram of CLMN treatment of MI. (E) NF-Kappa B signal pathway diagram.

pounds were compared with those of the positive control. The results showed that the target *RELA* had good binding activity with puerarin, ferulic acid, and daidzein. *IKBKB* had good binding activity with chrysin and galangin, and *NFKBIA* had good binding activity with puerarin. In addition, the conformation of the combination was stable, indicating that these may be the key components and targets of CLMN in the treatment of MI.

4.8 Composition of infiltrating immune cells in the peripheral blood of the GEO expression array data set

The GEO expression array data were used to investigate the proportion of infiltrated immune cells in the peripheral blood of MI patients. All of the 41 samples met the conditions of CIBERSORT ($p < 0.05$). As shown in Fig. 6, when myocardial infarction occurred, the body's immune inflammatory response was activated, which was manifested as an increased proportion of neutrophils and M0 macrophages and a decreased proportion of T cells, CD8, and T cells gamma delta. The infiltration rate of neutrophils in the peripheral blood of MI was the highest.

4.9 Quality control analysis

4.9.1 Chromatographic condition

By utilizing network pharmacology screening and a literature review to obtain the high-content medicinal ingredients and then according to the "Chinese Pharmacopoeia" 2020 edition regulations, puerarin, daidzein, 3'-

Table 1. Docking scores of target proteins with their corresponding compounds and positive controls.

Key target	Small molecule ligand	Docking score	Positive for drugs	Docking score
RELA	ferulic acid	101.9897	SC-236	105.787
	daidzein	98.4975		
	puerarin	108.584		
IKBKA	chrysin	102.312	Auranofin	99.9923
	galangin	98.5631		
NFKBIA	puerarin	98.3206	Astaxanthin	101.948

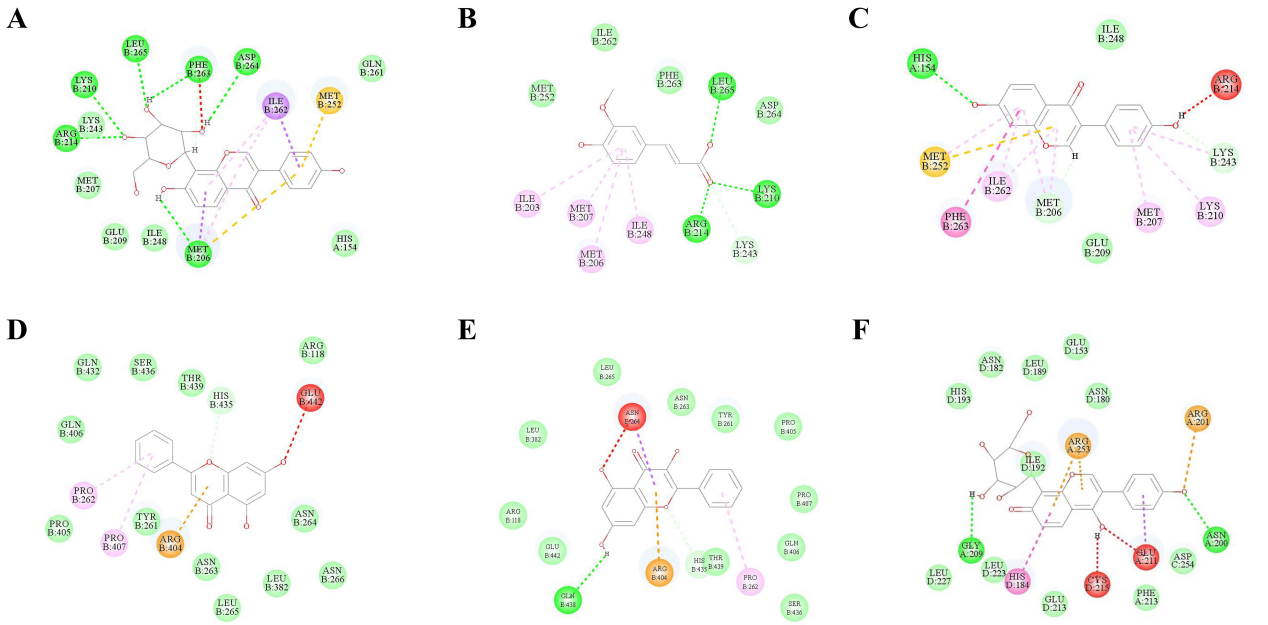

Fig. 5. Docking results of key target proteins with their corresponding compounds. (A) *RELA* and puerarin interaction diagram. (B) *RELA* and ferulic acid interaction diagram. (C) *RELA* and daidzein interaction diagram. (D) *IKBKB* and chrysin interaction diagram. (E) *IKBKB* and galangin interaction diagram. (F) *NFKBIA* and puerarin interaction diagram.

methoxydaidzein in *P. lobate*, dioscin in *D. nipponica Makino*, tetramethylpyrazine and ferulic acid in *L. wallichii*, and chrysin and galangin in propolis were selected as quality control standard samples. First, 1 mL of concentrated CLMN solution was volatized to 5 mL in methanol to obtain the test solution. puerarin, daidzein, 3'-methoxydaidzein, dioscin, tetramethylpyrazine, and ferulic acid, chrysin, and galangin reference substances were accurately weighed and placed in a 25-mL volumetric flask, dissolved in a solution of phosphoric acid-water:acetonitrile = 95:5, shaken well, and the volume was fixed to obtain the mixed reference substance solution. All of the samples were analyzed on an Agilent column (4.6 × 250 mm) using the mobile phase (phase A: phosphoric acid and water; phase B: acetonitrile) by gradient elution (Table 2). The detection wavelength was 203 nm, the volume flow rate was 1 mL/min, the column temperature was 30 °C, and the injection volume was 10 μL. By detecting and comparing the peak time of the test sample and the standard sample, the chromatogram of CLMN identified puerarin, daidzein, 3'-methoxydaidzein, dioscin, tetramethylpyrazine, ferulic acid, chrysin, and galangin, and established the quality standard of CLMN. As shown in Fig. 7 [27], the CLMN decoction contained the above eight compounds.

Table 2. Gradient elution program.

Time	Phosphoric acid - water/%	Acetonitrile/%
0	95	5
9	93	7
27	90	10
45	87	13
50	85	15
65	76	24
73	65	35
85	49	51
98	49	51
110	35	65
115	95	5
130	95	5

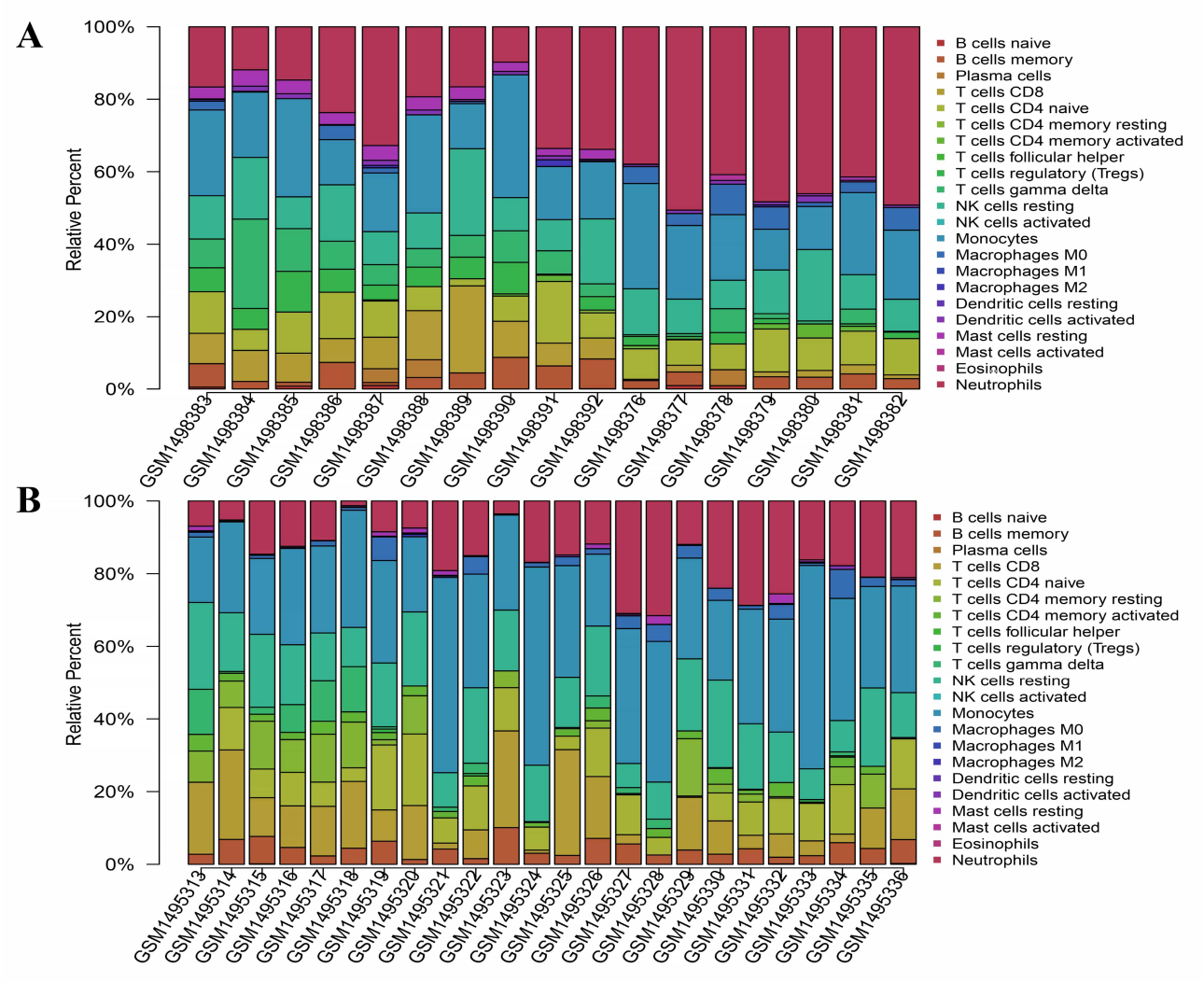

Fig. 6. The ratio of 22 immune cell subgroups in the peripheral blood of normal and MI patients. (A) GSE61145 expression array data set. (B) GSE60993 expression array data set. X axis: each GEO sample; Y axis: the percentage of each type of immune cell.

4.9.2 Investigation of linear RELAtionship

A total of 8 mg of puerarin, 1.6 mg of ferulic acid, 1.6 mg of tetramethylpyrazine, 0.48 mg of 3'-methoxydaidzein, 0.08 mg of chrysin, 0.16 mg of galangin, 0.16 mg of dioscin, and 1.6 mg of daidzein were accurately weighed and placed in a 10 mL volumetric flask. Phosphoric acid-water: acetonitrile = 95:5 solution standard, was added to a constant volume, shaken well, and set aside. The mother liquor 1 was absorbed into 0.5, 0.25, 0.125, 0.0625, and 2 mL volumetric flasks, and the volume was adjusted using phosphoric acid-water, acetonitrile = 95:5 solution to the scale, and then shaken well. Low to high concentrations of the mixed reference solution were injected into the liquid chromatograph, and the peak areas were recorded. The x-coordinate (X) was the concentration, and the y-coordinate (Y) was the peak area. The regression equation of each reference is shown in Table 3 below.

4.9.3 Sample content determination

Samples to be tested were collected and determined according to the method under "4.9.1" to obtain the content of the effective components of the CLMN. The results are shown in Table 4 below.

4.10 HE staining results

The results of the HE staining are shown in Fig. 8. The structure of the cardiomyocytes in the sham operation group was normal and orderly, with no pathological changes. However, in the MI model group, the cardiomyocytes were injured and disordered, with a large number of inflammatory cell infiltrates, and large areas of myocardial infarction and myocardial fibrosis. With the low dose of CLMN, more inflammatory cell infiltrates were observed. However, in the CDDP group, with the middle and high dose groups of CLMN, inflammation was alleviated, the area of myocardial infarction was significantly reduced, and cardiomyocyte fibrosis was inhibited.

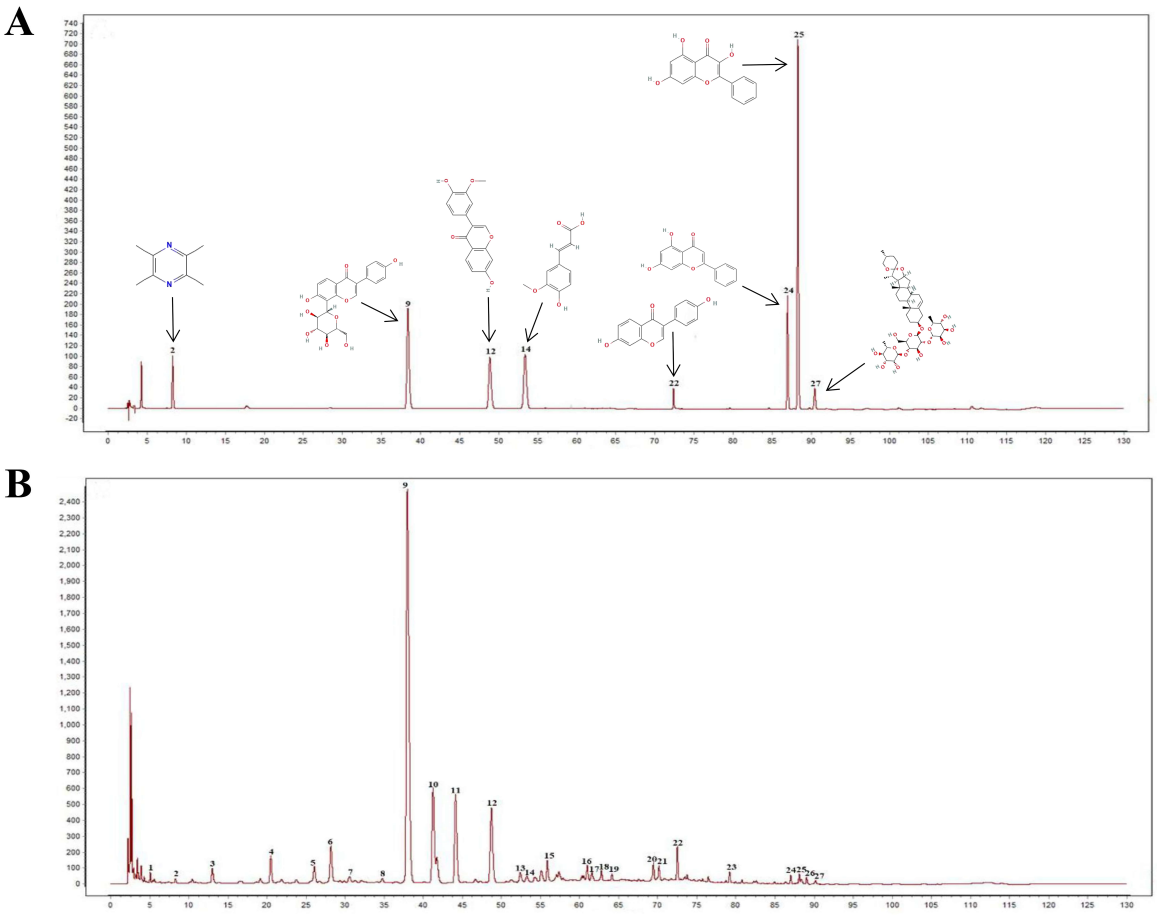

Fig. 7. Quality control of CLMN. (A) mixed reference substance. (B) CLMN fingerprint (No. 2: tetramethylpyrazine; No. 9: puerarin; No. 12: 3'-methoxydaidzein; No. 14: ferulic acid; No. 22: daidzein; No. 24: chrysin; 25: galangin; 27: dioscin).

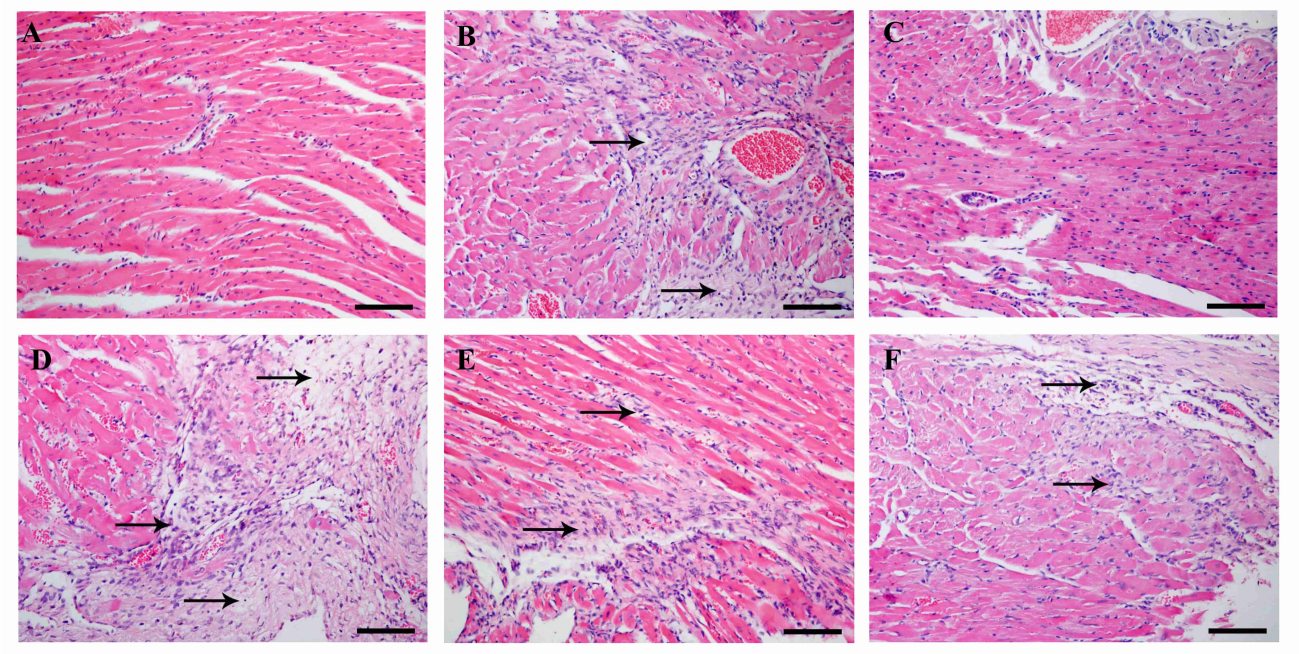

Fig. 8. The effect of CLMN on the pathomorphology of myocardial tissue in rats (HE, ×200). (A) Sham operation group. (B) Model group. (C) CDDP group. (D) CLMN low dose group. (E) CLMN medium dose group. (F) CLMN high dose group.

Table 3. Reference regression equation and linear range.

Reference substance	Regression equation	R^2 cor*RELA*tion coefficient	Linear range (μg/mL)
Puerarin	Y = 0.2017 X-0.8851	R^2 = 0.9999	25∼800
Tetramethylpyrazine	Y = 1.4085 X-0.3883	R^2 = 0.9998	5∼160
Ferulic acid	Y = 0.6873 X-0.1697	R^2 = 0.9992	5∼160
3'-methoxydaidzein	Y = 6.5348 X-4.5597	R^2 = 0.9998	3∼48
Daidzein	Y = 2.0826 X-0.4641	R^2 = 0.9995	5∼160
Chrysin	Y = 8.1272 X-0.3142	R^2 = 0.9998	0.25∼8
Galangin	Y = 11.579 X-1.0619	R^2 = 0.9998	0.5∼16
Dioscin	Y = 4.7049 X-1.6344	R^2 = 0.9981	0.5∼16

Table 4. Content determination result.

Components	Content (mg/g)
Puerarin	30.1145
Tetramethylpyrazine	0.1874
Ferulic acid	0.1796
3'-methoxydaidzein	8.1933
Daidzein	1.2249
Chrysin	0.8966
Galangin	0.9688
Dioscin	0.3522

4.11 *TNF-α*, *TRAF-2* and *IkBα* proteins in myocardial infarctions

The results of the immunohistochemical staining (Fig. 9) showed that compared with the sham group, the expression of the *TNF-α* and *TRAF-2* proteins were increased in the model group, while the protein expression level of *IkBα* was significantly decreased ($p < 0.05$). Compared with model group, in the CDDP group, the middle and high dose groups of CLMN significantly decreased the expression of the *TNF-α* and *TRAF-2* proteins and increased the expression level of the *IkBα* protein ($p < 0.05$).

5. Discussion

MI causes an inflammatory response mediated by cytokines [28], that may decrease myocardial contractile function and lead to myocardial hypertrophy, fibrosis and remodeling. The study is essential to repair an infarcted heart. Therefore, the regulatory mechanism of the inflammatory response urgently needs to be clarified, and its mechanism of action is still under exploration. In this study, based upon network pharmacology combined with the GEO chip, 52 core targets of CLMN were screened, and the results of the docking between the core targets and active components selected by the molecular docking software were stable. An MI mouse model was established, and the three targets of *TNF*, *TRAF-2*, and *NFKBIA* on the classical NF-Kappa B inflammatory signaling pathway were verified using the immunohistochemistry method. We demonstrated that *TNF-α* and *TRAF-2* were significantly decreased, and the expression level of the *IkBα* (*NFKBIA*) protein was significantly increased in the myocardium of mice treated with CLMN ($p < 0.05$).

A PPI network analysis showed that *MAPK1*, *STAT3*, *MMP9*, *MAPK14*, and other target genes had large degrees of freedom, and these may be the key targets of CLMN in the treatment of MI. Target proteins appear to be related and combine to produce the synergistic effect of CLMN. *MAPK1* is involved in a variety of cellular processes such as proliferation, differentiation, and transcriptional regulation [29]. Zhao *et al*. [30] showed that berberine down-regulates the p38MAPK-mediated NF-Kappa signaling pathway, thereby increasing the expression of inflammatory cytokines. Previous studies have indicated that phosphorylated *STAT3* activates the NF-Kappa B signaling pathway, and the transcription factor, NF-KB, enters the nucleus from the cytoplasm, thus regulating the expression of inflammatory cytokines [31]. *MMP9* is primarily regulated by the gene transcription level. There are multiple transcription factor binding sites, such as nuclear factor NF-KB, in the promoter of the *MMP9* gene [32], and NF-KB can enhance the expression of *MMP9*, which in turn plays an important role in the occurrence and development of coronary heart disease [33]. A large number of studies have shown that *MAPK14* activity plays a crucial role in the body's inflammatory response and is closely related to cardiovascular disease. When *MAPK14* is activated, it initiates an inflammatory cascade, further phosphorylates the downstream protein kinases and transcription factors, and then up-regulates the expression of *TNF-α* and other inflammatory factors [34]. Based on the above analysis, *STAT3*, *MMP9*, *MAPK14*, *NFKBIA*, and other targets may participate in the anti-inflammatory effect of CLMN by regulating the NF-Kappa signaling pathway. There are 37 components in CLMN may have therapeutic effects on MI. Some active components have been screened by network pharmacology combined with molecular docking technology, and puerarin, ferulic acid, daidzein, and others have been shown to have pharmacological effects against MI. Ferulic acid can inhibit the expression of E-selectin and P-selectin in endothelial cells, slightly inhibit the expression

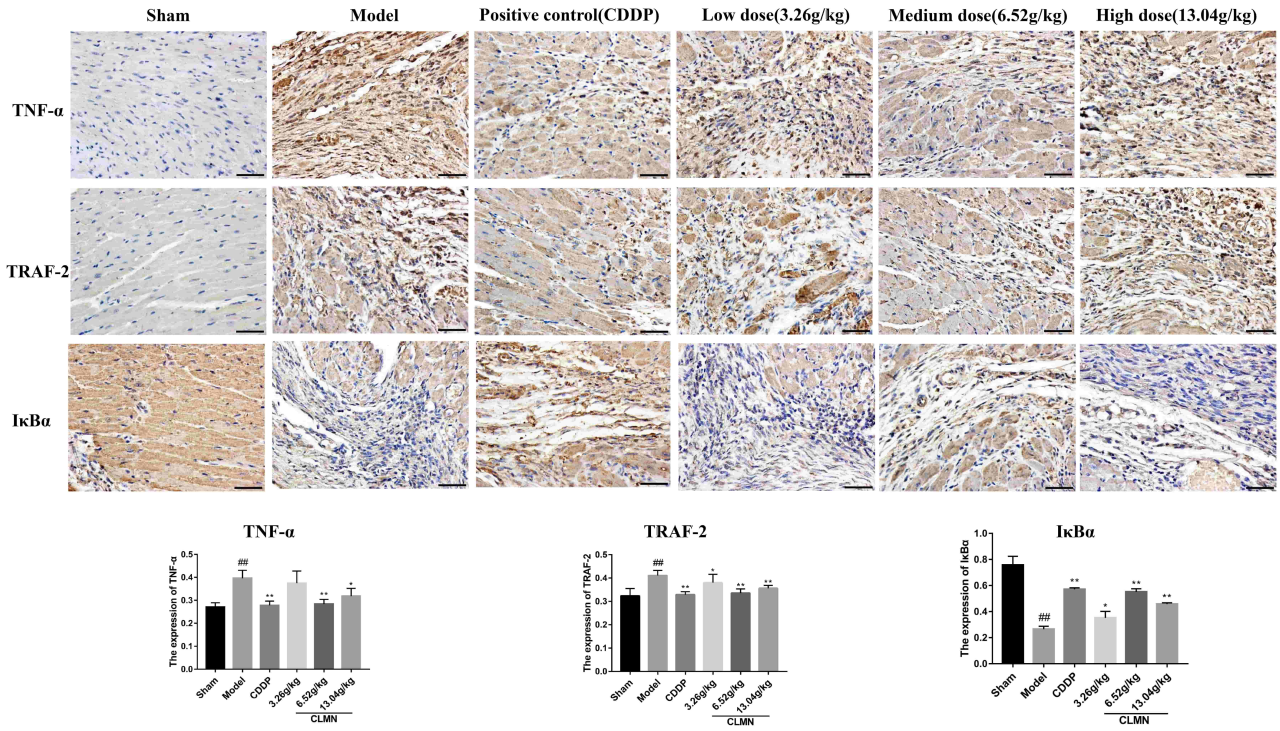

Fig. 9. Effects of CLMN Pretreatment on the expression of *TNF-α, TRAF-2, IkBα* protein in Myocardial tissue of mice with MI (Immunohistochemistry, ×400) and the changes of *TNF-α, TRAF-2, IkBα* protein expression in Myocardial tissue of mice.

of *VCAM-1*, and inhibit the release of vWF in endothelial cells, thus inhibiting the expression of adhesion molecules in endothelial cells and exerting an anti-atherosclerosis effect [35]. Daidzein can resist arrhythmia induced by myocardial ischemia/reperfusion injury and can significantly reduce the size of a myocardial infarction [36]. The HPLC analysis results showed that puerarin in the CLMN content was the highest. puerarin can relieve the inflammatory response in the myocardial cells to protect myocardial cells. In addition, puerarin can promote nitrogen oxide (NO) release from myocardial cells with vascular active substances, increase blood flow to the heart's blood vessels, and avoid myocardial injury caused by continuous ischemia [37].

The biological process enrichment analysis of CLMN showed that target-related biological processes areprimarily involved in the cellular response to chemical stress, the response to oxidative stress, and the regulation of reactive oxygen species metabolic process. The enrichment pathway of KEGG suggested the important involvement of Th17 cell differentiation, NF- Kappa B and other inflammatory signaling pathways, which supports the observation that the pathogenesis of MI is related to inflammation. *TNF-α* is considered to be one of the most important inflammatory cytokines [38]. Mature cardiomyocytes have the ability to produce *TNF-α* and its proteins under some stress-related conditions, and *TNF-α* can directly affect cardiac function and participate in a variety of cardiovascular pathological processes [39]. Based on the results of the analysis using the network pharmacology in this study and a review of the literature, we speculated that CLMN might treat MI by regulating the NF-Kappa B signaling pathway. Hence, we utilized immunohistochemistry to determine the expression levels of *TNF-a*, *TRAF2*, and *IkBα* proteins seven days after modeling and quantified their expression results according to the gray values. The NF-Kappa B pathway is the most thoroughly studied signal transduction pathway in the development of inflammation. The NF-Kappa B signal pathway is triggered by activated *TNF-α*. *TNF-α* activates NF-KB by binding to the TNF-R1 receptor and the TNF receptor to the dead zone, *TRAF2*, and serine/threonine kinase RIP. In the activated NF-Kappa B signal pathway, after *IkBα* is phosphorylated, the nuclear localization signal on NF-KB is exposed, and NF-KB enters the nucleus from the cytoplasm and binds to the KB site on the regulatory gene promoter to induce the transcription of the target gene. This induces a large number of inflammatory cytokines to participate in the inflammatory response [40]. *IkBα* is a key protein in the NF-Kappa B pathway that is necessary for the activation of NF-KB mediated by *TNF-α*. It is the main regulatory inhibitory protein of NF-KB (p50-p65) *in vivo*. There is a KB site in the promoter of the *IkBα* gene, so its synthesis is also regulated by NF-KB, thus forming a negative feedback regulation of NF-KB. The results of the immunohistochemistry showed that the CLMN decoction significantly decreased the expression of *TNF-α* and *TRAF2* and increased the expression of the *IkBα* pro-

tein. Therefore, the CLMN decoction may primarily target the NF-Kappa B pathway.

The CIBERSORT algorithm and ggplot2 package analysis showed that neutrophils, macrophages, T cells, and other immune cells played a key role in the development of MI. Neutrophils play a dual role in the pathophysic process following MI. In the early stage after MI, the pro-inflammatory type neutrophils have a strong pro-inflammatory and pro-injury effect. As time goes by, the proportion of the anti-inflammatory type increases, participating in the "damage repair response" after MI and playing an anti-inflammatory and anti-injury role [41]. Macrophages are one of the major cell types involved in the inflammatory response after myocardial infarction, and they can regulate heart regeneration by triggering the inflammatory response. Studies have shown that after heart damage, neonatal mice can selectively expand MHC-II^{low}CCR2^{-} resident macrophages in the heart to produce a small inflammatory response, induce angiogenesis and cardiomyocyte proliferation, and promote heart regeneration. Adult mice are affected. The damaged heart primarily recruits MHC-II^{high}CCR2^{+} macrophages that trigger lasting inflammatory responses and lead to cardiac fibrosis [42].

A certain chemical component of Chinese medicine cannot reflect the quality of Chinese medicine. All Chinese medicine acts through a synergistic effect of multiple components and targets. In this study, the quality of Chinese medicine was evaluated using the method of content determination. In this study, we screened eight potential pharmacodynamic components in the CLMN decoction, including puerarin, daidzein, 3'-methoxydaidzein, dioscin, tetramethylpyrazine, ferulic acid, chrysin, and galangin. The quality standard of CLMN was established, and the eight effective components were determined. The content determination of the multi-index components in the CLMN decoction established in this experiment can be used for quality control of the substance reference of CLMN.

In summary, this study systematically studied the mechanism of CLMN for the treatment of MI. CLMN may regulate the NF-Kappa B signaling pathway and the expression of *RELA*, *IKBKB*, *NFKBIA*, and other targets in the pathway for treating MI through the active components such as puerarin, daidzein, ferulic acid, galangin, and chrysin. CLMN treatment of MI is a process involving multiple-components, multiple targets, and multiple pathways. This study not only provides a new explanation for the "multi-component, multi-target, and multi-pathway" effect of CLMN treatment of MI, but also screens out some major active compounds of CLMN and establishes the quality standard of the CLMN decoction. In addition, the CIBERSORT algorithm was also used to evaluate the immune cell infiltration in MI, and the three targets of *TNF-a*, *TRAF-2*, and *NFKBIA* on the classic inflammatory pathway NF-Kappa B pathway were verified. The study demonstrated that TCM, CLMN in particular, has diverse pharmacologically active components, that may act synergistically to provide treatment for MI.

6. Conclusions

In this study, network pharmacology and experimental validation were combined to explore the potential mechanism of CLMN in the treatment of MI. CLMN can effectively decrease the expression of *TNF-*α and *TRAF-2*, as well as increase the expression of *IkB*α, thereby CLMN might treat MI by regulating the NF-Kappa B signaling pathway. This study provides a basis for active ingredients and further mechanistic research on CLMN in the treatment of MI.

7. Author contributions

JL, XW and DB performed the data analysis, wrote the first version of the manuscript and processed the graph and the table in the manuscript. JBZ, SX, YW and YJ finalized the manuscript. SY, WW, JHZ and JH collected the data. XZ and CW (corresponding author) conceived and coordinated the study. All authors read and approved the final manuscript.

8. Ethics approval and consent to participate

The experimental animals were obtained with the informed consent of all participants. The institutional review board of the Shaanxi University of Chinese Medicine approved this experimental, code SYXK (chuan) 2020-030.

9. Acknowledgment

Thanks to all the peer reviewers for their opinions and suggestions.

10. Funding

This work was supported by Engineering and Technology Research Center for Application and Development of Chinese Herbal Medicine in Qinling, Shaanxi Province (20082DGC-32), the National Natural Science Foundation of China (Grant no. 81373944), Discipline Innovation team Project of Shaanxi University of Chinese Medicine (2019-YL11), Shaanxi University of Traditional Chinese Medicine, the key technology innovation team for the integration of traditional Chinese medicine (2018TD-005), Scientific Research in the affiliated Hospital of Shaanxi University of Chinese Medicine (2020ZJ005) and Shaanxi Provincial Key Research and Development Program (2017SF-351).

11. Conflict of interest

The authors declare no conflict of interest.

12. References

[1] Hu SS. Report on cardiovascular health and diseases In Chinese 2019: An updated summary. Chinese Circulation Journal. 2020; 35: 833–854.

[2] Benjamin EJ, Muntner P, Alonso A, Bittencourt MS, Callaway CW, Carson AP, *et al*. Heart Disease and Stroke Statistics-2019 Update: A Report From the American Heart Association. Circulation. 2019; 139: e56-e528.

[3] Okwuosa IS, Lewsey SC, Adesiyun T, Blumenthal RS, Yancy CW. Worldwide disparities in cardiovascular disease: Challenges and solutions. International Journal of Cardiology. 2016; 202: 433–440.

[4] Hu WX, Zhang XL, Xuan L, Chen MM, Zhang H. Correlation between serum C1q tumor necrosis factor-related protein 4 and high-sensitivity C-reactive protein levels and coronary heart disease. Journal of Hainan Medical University. 2021; 27: 338-343. (In Chinese)

[5] Wang J, Zhao CB, Tang JQ, Bu DD, Zou JB, Zhang XF, *et al*. Simultaneous determination of 7 components in compound Longmaining by HPLC. Central South Pharmacy. 2020; 18: 1903–1905. (In Chinese)

[6] Wang CL, Wang S, Shi YJ, Wang PQ. Pharmacodynamics Experiment of Fufang Longmaining Different Ratios. Journal of Liaoning University of Traditional Chinese Medicine. 2014; 16: 7–11. (In Chinese)

[7] Hopkins AL. Network pharmacology: the next paradigm in drug discovery. Nature Chemical Biology. 2008; 4: 682–690.

[8] Yuan C, Wang M, Wang F, Chen P, Ke X, Yu B, *et al*. Network pharmacology and molecular docking reveal the mechanism of Scopoletin against non-small cell lung cancer. Life Sciences. 2021; 270: 119105.

[9] Ru J, Li P, Wang J, Zhou W, Li B, Huang C, *et al*. TCMSP: a database of systems pharmacology for drug discovery from herbal medicines. Journal of Cheminformatics. 2014; 6: 13.

[10] Xu X, Zhang W, Huang C, Li Y, Yu H, Wang Y, *et al*. A novel chemometric method for the prediction of human oral bioavailability. International Journal of Molecular Sciences. 2012; 13: 6964–6982.

[11] Consortium TU, Alex B, Maria-Jesus M, Sandra O, Michele M, Rahat A, *et al*. UniProt: the universal protein knowledgebase in 2021. Nucleic Acids Research. 2021; 49: D480–D489.

[12] Kim S, Chen J, Cheng T, Gindulyte A, He J, He S, *et al*. PubChem in 2021: new data content and improved web interfaces. Nucleic Acids Research. 2021; 49: D1388–D1395.

[13] Gfeller D, Michielin O, Zoete V. Shaping the interaction landscape of bioactive molecules. Bioinformatics. 2013; 29: 3073–3079.

[14] Stelzer G, Dalah I, Stein TI, Satanower Y, Rosen N, Nativ N, *et al*. In-silico human genomics with GeneCards. Human Genomics. 2011; 5: 709–717.

[15] Edgar R. Gene Expression Omnibus: NCBI gene expression and hybridization array data repository. Nucleic Acids Research. 2002; 30: 207–210.

[16] Ritchie ME, Phipson B, Wu D, Hu Y, Law CW, Shi W, *et al*. Limma powers differential expression analyses for RNA-sequencing and microarray studies. Nucleic Acids Research. 2015; 43: e47.

[17] Khomtchouk BB, Van Booven DJ, Wahlestedt C. HeatmapGenerator: high performance RNAseq and microarray visualization software suite to examine differential gene expression levels using an R and C++ hybrid computational pipeline. Source Code for Biology and Medicine. 2014; 9: 30.

[18] Szklarczyk D, Gable AL, Lyon D, Junge A, Wyder S, Huerta-Cepas J, *et al*. STRING v11: protein–protein association networks with increased coverage, supporting functional discovery in genome-wide experimental datasets. Nucleic Acids Research. 2019; 47: D607–D613.

[19] Kohl M, Wiese S, Warscheid B. Cytoscape: Software for Visualization and Analysis of Biological Networks. Methods in Molecular Biology. 2011; 13: 291–303.

[20] Yu G, Wang L, Han Y, He Q. ClusterProfiler: an R Package for Comparing Biological Themes among Gene Clusters. OMICS: a Journal of Integrative Biology. 2012; 16: 284–287.

[21] Burley SK, Bhikadiya C, Bi C, Bittrich S, Chen L, Crichlow GV, *et al*. RCSB Protein Data Bank: powerful new tools for exploring 3D structures of biological macromolecules for basic and applied research and education in fundamental biology, biomedicine, biotechnology, bioengineering and energy sciences. Nucleic Acids Research. 2021; 49: D437–D451.

[22] Chen B, Khodadoust MS, Liu CL, Newman AM, Alizadeh AA. Profiling Tumor Infiltrating Immune Cells with CIBERSORT. Methods in Molecular Biology. 2018; 1711: 243–259.

[23] Ginestet C. Ggplot2: Elegant Graphics for Data Analysis. Journal of the Royal Statistical Society: Series a (Statistics in Society). 2011; 174: 245–246.

[24] Wang S, Wang CL, Shi YJ. HPLC Fingerprint of Fufang Longmaining Decoction. Chinese Archives of Traditional Chinese Medicine. 2015; 33: 89–92 + 9–10. (In Chinese)

[25] Gouweleeuw L, Hovens IB, Liu H, Naudé PJW, Schoemaker RG. Differences in the association between behavior and neutrophil gelatinase-associated lipocalin in male and female rats after coronary artery ligation. Physiology & Behavior. 2016; 163: 7–16.

[26] Lin W, Lo L, Chen H, Lai C, Yamada S, Liu S, *et al*. Sleep-*RELA*ted changes in cardiovascular autonomic regulation in left coronary artery ligation rats: Neural mechanism facilitating arrhythmia after myocardial infarction. International Journal of Cardiology. 2016; 225: 65–72.

[27] Chen M, Lin LF, Liu YL, Wang CM, Li H, Yang YJ. Establishment of HPLC fingerprint and determination of three components of classical Linggui Zhugan Decoction. Chinese Traditional and Herbal Drugs, 2019; 50: 4152-4157. (In Chinese)

[28] Gao R, Li X, Xiang H, Yang H, Lv C, Sun X, *et al*. The covalent NLRP3-inflammasome inhibitor Oridonin relieves myocardial infarction induced myocardial fibrosis and cardiac remodeling in mice. International Immunopharmacology. 2020; 90: 107133.

[29] Gu N, Ge K, Hao C, Ji Y, Li H, Guo Y. Neuregulin1β Effects on Brain Tissue via ERK5-Dependent MAPK Pathway in a Rat Model of Cerebral Ischemia-Reperfusion Injury. Journal of Molecular Neuroscience. 2017; 61: 607–616.

[30] Hutton SR, Otis JM, Kim EM, Lamsal Y, Stuber GD, Snider WD. ERK/MAPK Signaling is Required for Pathway-Specific Striatal Motor Functions. The Journal of Neuroscience. 2017; 37: 8102–8115.

[31] Pitman H, Innes BA, Robson SC, Bulmer JN, Lash GE. Altered expression of interleukin-6, interleukin-8 and their receptors in decidua of women with sporadic miscarriage. Human Reproduction. 2013; 28: 2075–2086.

[32] Zhang B, Henney A, Eriksson P, Hamsten A, Watkins H, Ye S. Genetic variation at the matrix metalloproteinase-9 locus on chromosome 20q12.2-13.1. Human Genetics. 1999; 105: 418–423.

[33] Gómez-Hernández A, Sánchez-Galán E, Ortego M, Martín-Ventura JL, Blanco-Colio LM, Tarín-Vicente N, *et al*. Effect of intensive atorvastatin therapy on prostaglandin E2 levels and metalloproteinase-9 activity in the plasma of patients with non-ST-elevation acute coronary syndrome. The American Journal of Cardiology. 2008; 102: 12–18.

[34] Roux PP, Blenis J. ERK and p38 MAPK-activated protein kinases: a family of protein kinases with diverse biological functions. Microbiology and Molecular Biology Reviews. 2004; 68: 320–344.

[35] Zhou Y, Li M, Sun QY. Effect of chlorogenic acid, caffeic acid, and ferulic acid on inhibition of nflammatory response of HMECs induced by activated complement alternative pathway. Chinese Pharmacological Bulletin. 2016; 32: 1723–1728. (In Chinese)
[36] Kuang Y, Sha MM, Ma HX, Ren JN, Rao BL, Xue WJ, *et al*. Effects of daidzein on I_Na in rat ventricular myocytes. Chinese Pharmacological Bulletin. 2019; 35: 71–77. (In Chinese)
[37] Liu T. Efficacy of puerarin on content of serum CRP, NO and CK in rats with myocardial ischemia reperfusion injury. Clinical Journal of Chinese Medicine. 2018; 10: 12–13. (In Chinese)
[38] Zhang X, Cui L, Chen B, Xiong Q, Zhan Y, Ye J, *et al*. Effect of chromium supplementation on hs-CRP, *TNF-*α and IL-6 as risk factor for cardiovascular diseases: a meta-analysis of randomized-controlled trials. Complementary Therapies in Clinical Practice. 2021; 42: 101291.
[39] Giroir BP, Horton JW, White DJ, McIntyre KL, Lin CQ. Inhibition of tumor necrosis factor prevents myocardial dysfunction during burn shock. the American Journal of Physiology. 1994; 267: H118–H124.
[40] Monika, Sharma A, Suthar SK, Aggarwal V, Lee HB, Sharma M. Synthesis of lantadene analogs with marked in vitro inhibition of lung adenocarcinoma and *TNF-*α induced nuclear factor-kappa B (NF-κB) activation. Bioorganic & Medicinal Chemistry Letters. 2014; 24: 3814–3818.
[41] Chen X, Liu XX, Xia H. Research progress of the role of neutrophils in myocardial infarction. Chinese Journal of Cardiovascular Medicine. 2020; 25: 389–392. (In Chinese)
[42] Wang LP, Chen R, Yan JC, Liu PJ. Research progress of macrophages in regeneration of different tissues. Chinese Journal of Pathophysiology. 2021; 37: 565–570. (In Chinese)

Abbreviations: MI, Myocardial Infarction; CLMN, Compound Longmaining; HE, hematoxylin-eosin; TCMs, Traditional Chinese medicines; DEGs, differentially expressed genes; TCMSP, Traditional Chinese Medicine Systems Pharmacology; OB, Oral Bioavailability; DL, Drug-likeness; PPI, protein-protein interaction; GO, Gene ontology; KEGG, Kyoto Encyclopedia of Genes and Genomes.

Keywords: Network pharmacology; Compound Longmaining decoction; Myocardial infarction; Immune cell infiltration; Quality control; NF-Kappa B signaling pathway

Send correspondence to:

Xiaofei Zhang, Department of Pharmaceutics, College of Pharmacy, Shaanxi University of Chinese Medicine, 712000 Xianyang, Shaanxi, China, E-mail: 2051028@sntcm.edu.cn

Changli Wang, Department of Pharmaceutics, College of Pharmacy, Shaanxi University of Chinese Medicine, 712000 Xianyang, Shaanxi, China, E-mail: wcl3433@163.com

† These authors contributed equally.